J Mater Sci (2007) 42:5442–5447
DOI 10.1007/s10853-006-0790-4

Fabrication and properties of in situ synthesized particles reinforced aluminum matrix composites of Al–Zr–O–B system

G. R. Li · Y. T. Zhao · Q. X. Dai · X. N. Cheng · H. M. Wang · G. Chen

Received: 22 March 2006 / Accepted: 11 August 2006 / Published online: 28 March 2007

Abstract A new in situ Al–Zr–O–B system is exploited. The Al–Zr$(CO_3)_2$–KBF_4 components are used to fabricate the particle reinforced aluminum matrix composites by the direct melt reaction method. The analytical results of XRD and SEM show that the in situ endogenetic particles are $ZrAl_3$, ZrB_2 and Al_2O_3, which are well distributed in the aluminum matrix. The sizes of reinforced particles are 0.5–2.5 μm. The results of mechanical properties of the composites show that the tensile strength and yield strength are improved with the increase of theoretical volume fraction of particles in matrix in the range of 0–12%, which are much superior to those of aluminum matrix. The best elongation of composites is 33% when the theoretical volume fraction is 3%. The fracture mechanism belongs to a ductile one. The wear resistance properties of the composites are much higher than that of aluminum matrix. The best abradability is got when the theoretical volume fraction of particles is 6%. The wear mechanism of the aluminum matrix is adhesive wear while the wear mechanism of $(ZrAl_3 + ZrB_2 + Al_2O_3)_p$/Al composites is abrasive wear.

Introduction

Over the past 20 years considerable attention has been paid to the particles reinforced metal matrix composites (PRMMCs), especially the aluminum matrix ones developed rapidly as a result of their good performances, such as high strength, high hardness, excellent wear resistance, low heat expansion coefficient, competitive cost and so on. The development of them has been driven by the aerospace, automotive industries and other structural applications to yield stronger and stiffer light metal matrix composites.

PRMMCs can be fabricated in two different major routes. One route is the addition of ceramic particulates to the matrix materials. It requires the preparation of reinforcing particulates prior to composite fabrication, which can be viewed as ex situ PRMMCs. In this case, the scale of the reinforcing phase is limited by the starting powder size, which is typically of the order of microns to tens of microns and rarely below 1 μm. The other is the in situ composites in which the reinforcements are synthesized in a metallic matrix by chemical reaction between elements or between element and compound during the composite fabrication. Compared to the ex situ composites the in situ PRMMCs exhibit the following advantages: (a) the reinforcement–matrix interfaces are clean, resulting in a strong interfacial bonding; (b) the in situ formed reinforcing particulates are finer in size and their distribution in the matrix is more uniform, yielding better mechanical properties. Using this route some techniques include self-propagating high temperature synthesis (SHS), exothermic dispersion (XD), vapor liquid synthesis (VLS), solid liquid synthesis (SLS), directed metal oxidation (DIMOX) and second phase particulates (including borides, carbides, nitrides, oxides and their mixtures) have been studied [1–9].

The purpose of present work is to exploit a novel Al–Zr–O–B system to synthesize a kind of in situ particle reinforced aluminum matrix composites by the direct melt reaction method between zirconium carbonate and potassium fluoborate with molten aluminum. The presumed

G. R. Li (✉) · Y. T. Zhao · Q. X. Dai · X. N. Cheng · H. M. Wang · G. Chen
School of Materials Science & Engineering, Jiangsu University, Zhenjiang, Jiangsu Province 212003, P.R. China
e-mail: whmlgr@ujs.edu.cn

reinforced particles are $ZrAl_3$, ZrB_2 and Al_2O_3. All of them have higher elastic modulus and stability, which tend to be effective reinforced phases. In addition more than one reinforced particles generate in matrix, the properties of the composites may exhibit unique characteristics. The microstructures, thermodynamic of in situ reaction, mechanical characteristics of tensile and yield strength and dry sliding wear properties were further investigated.

Experimental procedure

Raw materials were aluminum ingot, zirconium carbonate ($Zr(CO_3)_2 \cdot mH_2O$) and potassium fluoborate powder ($KBF_4 \cdot nH_2O$). Zirconium carbonate and potassium fluoborate powder were pre-heated to dehydrate the bounded water in electric oven at 250 °C for 3 h. Then the dried $Zr(CO_3)_2$ and KBF_4 powder were cooled, grounded and screened .At the same time, aluminum ingot was molten in an electric furnace under an argon atmosphere and held at 850 °C. Certain amount of dehydrated reactants powder was added and incorporated with mechanical stirring. The expected volume content (%) of reinforced phases formed in composites was listed in Table 1. Due to the kinetic condition the in situ reaction could not proceed sufficiently, so the actual volume fractions of particles were often less than the calculated theoretical values. Average recovery rate was about 60–80%, which was decreased with the increase of adding amount of reactants. During the process the in situ reinforced particulates were formed in the molten aluminum. After 30 min inspired gases were degassed and extra solid substances were removed by refining slag. Subsequently the melt was cast into a permanent mould at 720 °C. To obtain the best fabrication conditions, L_9 (3^4) orthogonal table was selected to design the experiments.

Tensile behavior of composites at room temperature was conducted on WD10 type electronic stretcher. The strain rate was 1×10^{-4}–1×10^{-1} s^{-1} and the sample shape was shown as Fig. 1. The sliding wear test was carried out under dry conditions using a block-on-disc wear testing machine. The specimen (in the form of a block: $19.5 \times 10 \times 8$ mm^3) was slid against a rotating 40Cr steel disc ($\varnothing 40 \times \varnothing 16 \times 10$ mm^3). The load, wear time and sliding speed were 90N, 90s and 0.42 m/s separately. The wear loss was determined from the difference of the sample between the initial and final weight after a specified time of wear. JEOL-JXA-840A scanning-electron microscope (SEM) was used to observe the morphology of reinforced phases, the pattern of tensile fracture and superficial features of wear samples. D/max2500 X-Ray Diffraction (XRD) was applied to analyze the kinds of reinforced phases. Furthermore the grain size of corroded samples by 0.5 wt.% HF was measured by MM-6 horizontal microscope.

Result and discussion

Microstructure of composites

Figure 2 is the XRD diagram of composites fabricated using Al–$Zr(CO_3)_2$–KBF_4 components. It shows that the

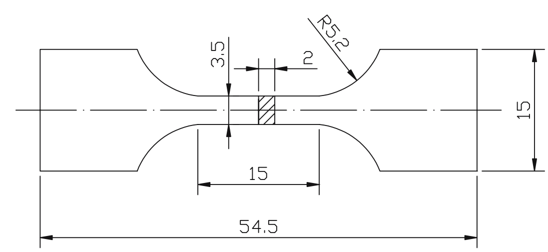

Fig. 1 Schematic illustration of the tensile specimen at room temperature

Table 1 Expected theoretical volume fractions (%) of reinforced phases in situ formed in samples

	Reactants			Resultants		
	12 Al	$2KBF_4$	$3\ Zr(CO_3)_2$	$2\ Al_2O_3$	$2\ ZrAl_3$	ZrB_2
Molecular weight in Eq. 5 and density (ρ) of substance	324 $\rho = 2.7$ g/cm^3	252	633	204 $\rho = 3.98$ g/cm^3	344 $\rho = 4.1$ g/cm^3	113 $\rho = 6.09$ g/cm^3
The calculation of adding x amount of reactants and output of resultants (g)	10% is a presumed weight percent	$\frac{252 \times 10\%}{324}x = 0.078x$	$\frac{633 \times 10\%}{324}x = 0.195x$	$\frac{204 \times 10\%}{324}x = 0.063x$	$\frac{344 \times 10\%}{324}x = 0.106x$	$\frac{113 \times 10\%}{324}x = 0.035x$
Theoretical volume fraction (TVF) (%)	$\frac{x}{2.7}$	–	–	$\frac{0.063 \times 2.7}{3.98} \times 100\% = 4.27\%$	$\frac{0.106 \times 2.7}{4.1} \times 100\% = 6.98\%$	$\frac{0.035 \times 2.7}{6.09} \times 100\% = 1.55\%$
Total TVF				12.8%		

Note: The adding amount of reactants corresponding to 3, 6, 9, 12% TVF can be calculated following the above proportions

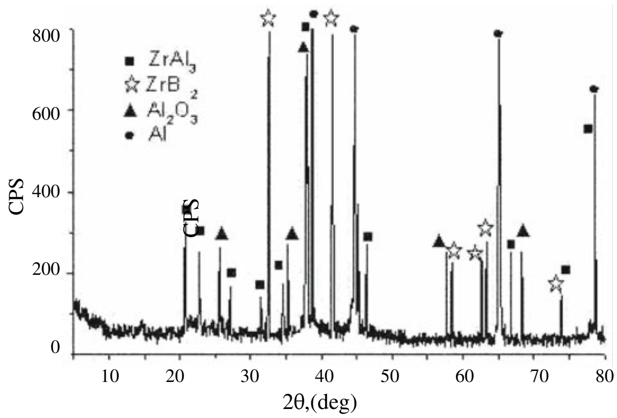

Fig. 2 XRD diagram of composites synthesized in Al–Zr–O–B system

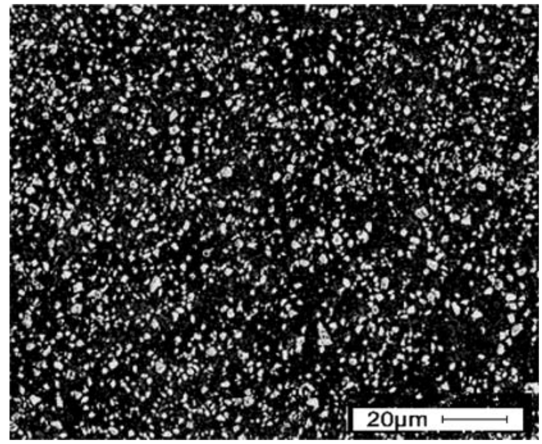

Fig. 3 SEM photomicrograph of composite synthesized in Al–Zr–O–B system

in situ formed reinforcements in Al–Zr–O–B system are $ZrAl_3$, ZrB_2 and Al_2O_3. Figure 3 illustrates the SEM microstructure of the composites, which indicates that the endogenous particulates are well distributed in Al matrix.

$$AlB_2 + ZrAl_3 = ZrB_2 + 4Al. \quad (4)$$

Basing on the date offered by references [10–12], the thermodynamic parameters are calculated:

$$\begin{aligned} \Delta G^{\Theta}_{ZrO_2} &= -1082151.4 + 198.52T, & \Delta G^{\Theta}_{Al} &= -5609.9 - 11.35T, \\ \Delta G^{\Theta}_{ZrAl_3} &= -25138.3 - 319.4T, & \Delta G^{\Theta}_{Al_2O_3} &= -1121951.3 + 323.124T, \\ \Delta G^{\Theta}_{AlB_2} &= 38730.4 - 69.80T, & \Delta G^{\Theta}_{ZrB_2} &= -318236 + 19.706T. \end{aligned}$$

Figure 4 shows the patterns of the three reinforced particles. $ZrAl_3$, ZrB_2 and Al_2O_3 exhibits irregular polygon, small hexagon and elliptical forms separately. The sizes of the particles are in the range of 0.5–2.5 μm. The technological parameters of in situ fabricating are evaluated in terms of particulate granularity and distribution state so as to compare the orthogonal experiment results and optimize the synthetic conditions. When the original reaction temperature is 870 °C, theoretical volume fraction is 12% and reaction time is 25 min, the corresponding microstructure of cast composites is excellent.

Thermodynamic analysis of in situ reaction

The metallurgical reactions between $Zr(CO_3)_2$, KBF_4 and molten Al are deduced as four intermediate steps

$$Zr(CO_3)_2 = ZrO_2 + CO_2 \quad (1)$$

$$2KBF_4 + 3Al = AlB_2 + 2KAlF_4 \quad (2)$$

$$ZrO_2 + 13Al = 3ZrAl_3 + 2Al_2O_3 \quad (3)$$

So the Gibbs free energy of reaction (3), (4) are:

$$\Delta G^{\Theta}_3 = -1000065.4 + 756T, \ \Delta G^{\Theta}_4 = -354267.7 + 343.8T.$$

The equilibrium temperature of them are 1322.8 K (1049.7 °C) and 1030.4 K (757.3 °C), respectively. Actually the measured temperature of reaction system varies from 870 to 1006.7 °C when the calculated ΔG^{Θ}_3 is negative. So reaction (3) can proceed spontaneously. Nevertheless the reaction (4) cannot proceed sufficiently. In XRD diagram the small amount of ZrB_2 verifies the assertion. The whole reaction is obtained as formula (5)

$$\begin{aligned} 2KBF_4 + 3Zr(CO_3)_2 + 12Al = 2KAlF_4 + 6CO_2 \\ \uparrow + 2Al_2O_3 + 2ZrAl_3 + ZrB_2. \end{aligned} \quad (5)$$

Tensile property of composites

The tensile properties at room temperature of the composites and pure Al were identically processed. The test results are given in Figs. 5, 6. Compared with pure Al the enhancements of the properties in terms of tensile strength (σ_b) and yield strength (σ_s) of the composites are obviously seen. Furthermore the mechanical properties are improved

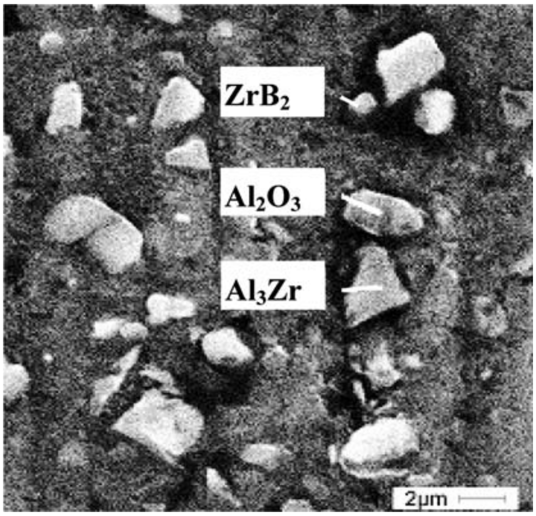

Fig. 4 Features of reinforced particles in the composites synthesized in Al–Zr–O–B system

with the increase of volume fraction of particles due to the in situ formed fine particles and uniform distribution in the matrix. When the theoretical volume fraction of particles is 12% the σ_b is 150.3 MPa, which is increased by 92.7% as compared to 78.0 MPa of pure Al, and the σ_s is 113.7 MPa, which is increased by 170.7% as compared to 42.0 MPa of pure Al.

The strengthening mechanisms may mainly include grain-refined strengthening and solid-solution strengthening.

(1) *Grain-refined strengthening*. $ZrAl_3$ is easy to be the nucleation basements of Al matrix, which can reduce the grain size of Al matrix significantly. According to the crystal structure analysis of $ZrAl_3$, the polyhedral particles can act as the catalyst for the heterogeneous nucleation of aluminum [13]. It was reported that there are matching location directions between $ZrAl_3$ and aluminum, as $(001)_{ZrAl_3}//[001]_{Al}$, $(001)_{ZrAl_3}//(001)_{Al}$. The misfit degree is only 0.95%.

(2) *Solid-solution strengthening*. When the foreign Zr atom dissolves in the Al matrix, it may act as an atomic-sized obstacle to the motion of dislocations. The solid solubility of Zr in aluminum is 0.28% at 660 °C according to Al–Zr binary phase diagram [14]. Because the volume of the Zr atom (2.33×10^{-11} m^3) is larger than that of the Al atom (1.66×10^{-11} m^3) a misfit strain field will be produced around the Zr atom that may interact with the dislocation strain field [15].

Figure 6 is the SEM apperarances of tensile fracture of the composites at room temperature. In Fig. 6a there are a variety of dimples and tearing edges on the fracture surface. The tearing edges are thin, dense and tangled. In Fig. 6b the amount of dimples and tearing edges decreased dramatically when the theoretical volume fraction of particles is increased from 3 to 12%, meanwhile the sizes of the dimples grow very significantly. The corresponding elongation decreased from 33 to 8.5%. Ductile fracture mechanism, not brittle one, of the composites is deduced from the appearances of tensile fracture.

Wear resistance of composites

The dry sliding wear characteristics of the $(ZrAl_3 + ZrB_2 + Al_2O_3)_p/Al$ composites is illustrated in Figs. 7, 8. Figure 7 shows the relationship between the theoretical volume fractions of particles and wear amount. When the theoretical volume fraction of particles is 6% the wear amount is only 58.2 mg, which is the lowest point on the

Fig. 5 Mechanical properties of $(ZrAl_3 + ZrB_2 + Al_2O_3)_p/Al$ composites

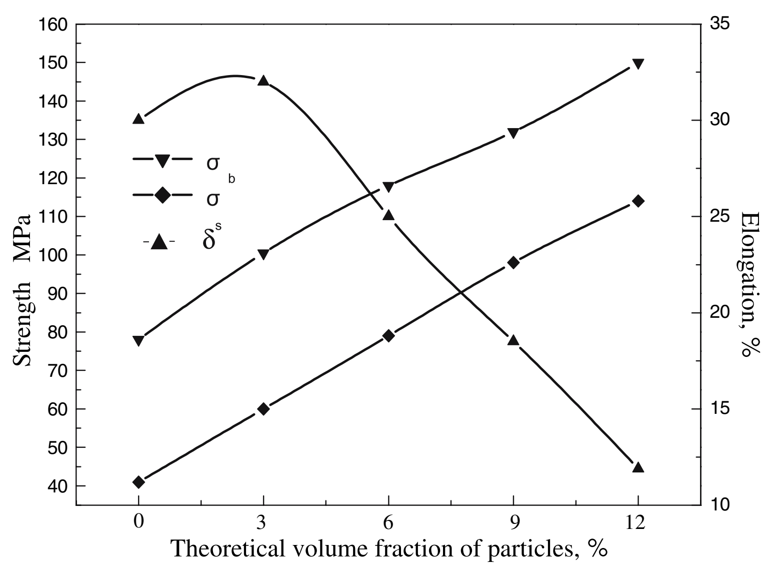

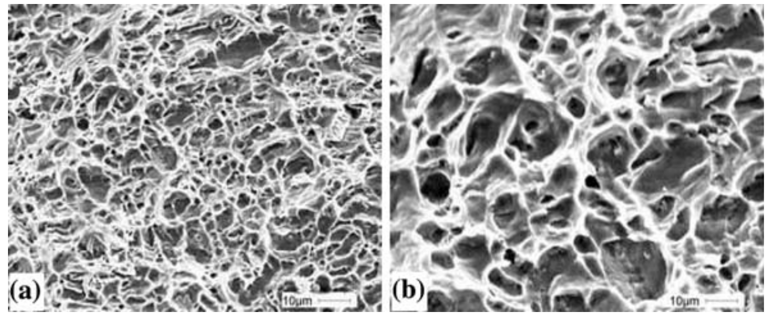

Fig. 6 Tensile fracture surfaces of $(ZrAl_3 + ZrB_2 + Al_2O_3)_p/Al$ composites at room temperature for 3% theoretical volume fraction of particles (**a**) and for 12% theoretical volume fraction particles (**b**)

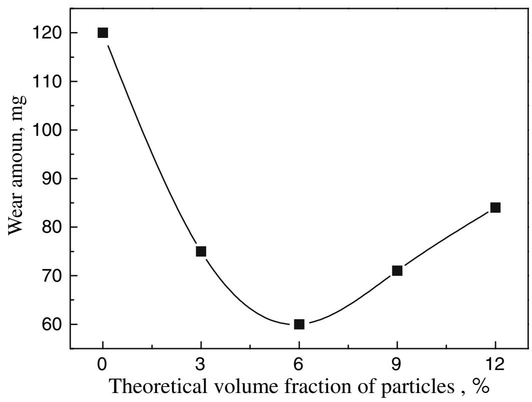

Fig. 7 Relationship between the theoretical volume fraction of particles and wear amount

parabolic curve. It is descended by 51.5% as compared to the 120 mg wear amount of pure Al.

Figure 8 is the SEM photographs of worn surfaces of Al matrix and composites. As shown in Fig. 8a there are serious deformations and stripped pits on the worn surface of Al matrix. The wear mechanism of the matrix Al is adhesive one. Figure 8b displays the relatively flat and smooth of the worn appearance of composites synthesized under the optimal conditions. Only several small and shallow pits can be seen. The reinforced particles extruding out of wear surface resist the destruction of 40Cr steel. Furthermore the plough trace can be seen obviously in Fig. 8b. It is presumed that some hard particles fall off from the surface and slide along the wear direction under the foreign force. It will aggravate the wear amount to a certain extent, as called ''plough effect''. The wear mechanism of $(ZrAl_3 + ZrB_2 + Al_2O_3)_p/Al$ composites is abrasive one.

Moreover, Fig. 7 shows that it is not the case that the composites fabricated with higher volume fraction of particles have better wear resistance because there are two sides to the effects of reinforced particles to influence the wear resistance of composites. In the composites both ZrB_2 and Al_2O_3 are hard ceramic particles. At 1,090 °C the elastic modulus of ZrB_2 and Al_2O_3 are 503 GPa and 379 MPa individually. They can increase the hardness and wear resistance of matrix. The theoretical volume fraction of ZrB_2 and Al_2O_3 is only 1.36% when the total theoretical volume fraction of particles is 3%, so small amount of endogenous particulates cannot sustain the wear efficiently. On the other hand plentiful particulates will prick up the plough effect (shown in Fig. 8b.). In this study the optimal volume fraction of particles is determined as 6% to get the best abradability when using $Al–Zr(CO_3)_2–KBF_4$ components to fabricate $(ZrAl_3 + ZrB_2 + Al_2O_3)_p/Al$ particulate reinforced composites.

Summary

(1) In this paper $Al–Zr(CO_3)_2–KBF_4$ components are used to fabricate the particle reinforced aluminum matrix composites by direct melt reaction method.

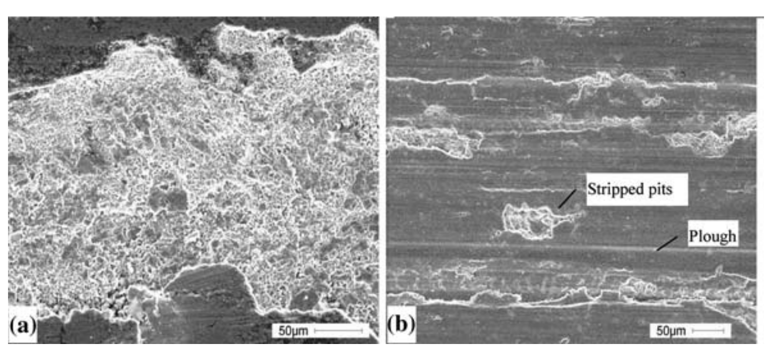

Fig. 8 SEM photomicrographs of worn surfaces of Al matrix (**a**) and $(ZrAl_3 + ZrB_2 + Al_2O_3)_p/Al$ composites synthesized under the optimal conditions (**b**)

The reinforced particles are $ZrAl_3$, ZrB_2 and Al_2O_3, which are well distributed in the matrix. The sizes of reinforced particles are 0.5–2.5 μm.

(2) The tensile strength and yield strength are improved with the increase of theoretical volume fraction of particulates in matrix in the range of 0–12%, which are much superior to that of aluminum matrix. The best elongation is 33% when the theoretical volume fraction is 3%. The fracture mechanism is a ductile one.

(3) The wear resistances of the composites are much higher than that of aluminum matrix. When the theoretical volume fraction of particles is 6% the composites have the best abradability. The wear mechanism of the aluminum matrix is adhesive wear while the wear mechanism of $(ZrAl_3 + ZrB_2 + Al_2O_3)_p$/Al composites is abrasive wear.

Acknowledgements The work is financially supported by High Technology and Industry Key Project of Jiangsu Province in China through research grant BG2005026 and BE2002039.

References

1. Cholewa M (2005) J Mater Pro Technol 164–165:1181
2. Tjong SC, Wang GS, Mai YW (2005) Compos Sci Technol 65:1537
3. Huang ZJ (2002) Acta Metallur Sin 6:568
4. Yu P, Mei Z, Tjiong SC (2005) Mater Chem Phy 93:109
5. Roy D, Ghosh S, Basumallick A, Basu B (2006) Mater Sci Eng A415:202
6. Zhao YT, Li ZH, Cheng XN et al (2003) Trans Nonferrous Met Soc China 13(4):669
7. Sun Zhiqiang, Zhang Di, Li Guobin (2005) Mater Design 26:454
8. Wang MM, Lu WJ, Qin JN et al (2006) Mater Design 27:494
9. Kok M (2006) Compos Part A 37:457
10. Li GR, Dai QX, Zhao YT (2005) Chin J Nonferrous Met 15(4):572
11. Li GR, Zhao YT, Dai QX (in press) J Univ Sci Technol
12. Zeng ZM (2003) Manual of mechanical engineering materials [M]. Mechanical industry publishing company, Peking
13. Zhao YT, Zhong ZH, Cheng XN et al (2003) Trans Nonferrous Met Soc China 12:770
14. Yu JQ, Yi YZ (1987) Atlas of binary alloy phases. Science publishing company, Shanghai
15. Verhoeven JD (1975) Fundamentals of physical metallurgy. John Wiley &Sons Inc, New York